Gillis, Richard B. and Adams, Gary G. and Alzahrani, Qushmua and Harding, Stephen E. and Allen Bush, C. (2016) A novel analytical ultracentrifugation based approach to the low resolution structure of gum arabic. Biopolymers, 105 (9). pp. 618-625. ISSN 1097-0282

A Novel Analytical Ultracentrifugation Based Approach to the Low Resolution Structure of Gum Arabic

Article *in* Biopolymers · February 2016

DOI: 10.1002/bip.22823

4 authors, including:

Richard B Gillis
University of Nottingham
28 PUBLICATIONS **101** CITATIONS
SEE PROFILE

Gary G Adams
University of Nottingham
96 PUBLICATIONS **711** CITATIONS
SEE PROFILE

Stephen Ernest Harding
University of Nottingham
491 PUBLICATIONS **8,221** CITATIONS
SEE PROFILE

A novel analytical ultracentrifugation based approach to the low resolution structure of gum Arabic

AUTHORS

Richard B. Gillis[1,2]*, Gary G. Adams[1,2], Qushmua Alzahrani[1,2], Stephen E. Harding[2]

[1] University of Nottingham, Faculty of Medicine and Health Science, Queens Medical Centre, NG7 2RD, UK

[2] University of Nottingham, National Centre for Macromolecular Hydrodynamics, School of Biosciences, Sutton Bonington Campus, Loughborough, LE12 5RD, UK

ABSTRACT

Under investigation are the structural properties of gum arabic, an industrially important biopolymer for use as a stabiliser or in drug delivery, using Analytical Ultracentrifugation – a well-established, matrix-free probe for macromolecular size and shape. These results are combined with chromatographically-coupled methods (multi-angle light scattering, differential press imbalance viscometry) to provide a global analysis of its structure in varying ionic strength conditions. This analysis indicates that gum Arabic may have a compact, elliptical structure in solution, the significance of which for biotechnological use is indicated. This modelling method can be applied to other biopolymers and synthetic polymers.

This article has been accepted for publication and undergone full peer review but has not been through the copyediting, typesetting, pagination and proofreading process which may lead to differences between this version and the Version of Record. Please cite this article as an 'Accepted Article', doi: 10.1002/bip.22823

KEYWORDS

Acacia, AUC, Characterisation, Conformation, Gum Arabic, Hydrodynamic, Sedimentation velocity, Ultracentrifugation

INTRODUCTION

Gum Arabic (GA), or acacia gum, is a glycoprotein which has applications in the food and pharmaceutical industries ranging from its emulsion-forming properties, its ability to form viscous solutions and its ability to bind with other macromolecules (1,2). It has also been reported to have multiple health benefits such as an anti-oxidant and a nephroprotectant (3).

The primary structures of both the sugar and protein fragments have been studied in detail (4). The polysaccharide component represents approximately 95% of the macromolecule and consists of a very complex, heavily branched β(1→3)D-galactopyranose backbone with a high proportion of arabinofuranose and rhamnopyranose residues (5) and terminal glucuronic acids. The protein component consists of a 250 amino acid chain, with regions of polysaccharide covalently O-linked to hydroxyproline and serine residues (6). This is often referred to as the wattle blossom model (3). In many ways, this model is similar in structure to mucous glycoproteins, which is also composed of a protein backbone with O-linked glycosylation to serine and threonine residues – a major difference between them being the saccharide chemical composition affecting the viscoelastic properties.

The overall hydrodynamic structure has previously been studied principally using light scattering and chromatographic based methods (6). From these, the "wattle blossom" model appears to have become favoured, with the overall conformation of the molecule being close to spherical. An alternative is the 'hairy rope' model (7) based on TEM imaging. It is also

tightly bound with Stokes radii between 5-30nm (9,10) and an intrinsic viscosity between 10-30ml/g. It is generally agreed that the weight average molar mass lies between 0.3- 2 MDa with a high degree of polydispersity (8), typical for an unfractionated polysaccharide. We now take a fresh look at the hydrodynamic structure of GA based around the powerful separation and analysis technique of sedimentation velocity in the analytical ultracentrifuge.

Analytical Ultracentrifugation (AUC) has the benefit of being 'matrix-free', requiring no columns or membranes which, particularly for charged polysaccharides such as GA (11), may cause complications with column-solute interaction. This study uses sedimentation velocity AUC (AUC-SV) in conjunction with size exclusion chromatography coupled to multi-angle (static) light scattering and differential viscometry (SEC-MALS-IV) to probe the hydrodynamic characteristics of GA from three different sources and solubilised under different ionic strengths.

MATERIALS

Gum Arabic was obtained from two suppliers: Branwell (Essex, UK) and Glycomix (Reading, UK) assigned GAB and GAG accordingly. Both samples were purified from the *Acacia senegal* crop and prepared into buffered solutions from spray-dried powder.

Samples were dissolved in phosphate buffered saline (pH 7.0). 0.05M of the buffer was disodium hydrogen orthophosphate dodecahydrate and potassium dihydrogen orthophosphate (Fisher Scientific, UK). Sodium chloride (Fisher Scientific, UK) was added to the buffer to increase ionic strengths to 0.1, 0.3 and 0.5M. 0.145ml/g was the refractive index increment used at 0.1M (12) and 0.150ml/g was assumed for 0.3 and 0.5M. These values are consistent with other recent publications (9,13).

METHODS

Density measurement

The concentration dependence of GA solution density was used to find the partial specific volume ($\bar{v}$), and provide supplementary density information for viscometry.

Sedimentation velocity in the Analytical Ultracentrifuge

Sedimentation velocity (AUC-SV) experiments were performed in a Beckman Optima XL-I Analytical Ultracentrifuge (Palo Alto, CA). Ultracentrifuge cells were assembled from 12mm, 2 channel aluminium epoxy resin centrepieces and sapphire windows in aluminium window holders. 400µl of sample (1-7mg/ml loading concentration) and corresponding buffer were injected into the cells, sealed and balanced. The rotor speed was set to 30 000 rev/min (~69 000 g), with Rayleigh Interference scans taken every minute.

Data analysis was performed using least squares g*(s) vs. s fitting in SEDFIT v14 (14). Apparent sedimentation coefficients (s), fringe concentration, and percentage content were taken by integrating the main peak. Sedimentation coefficients obtained in the buffer were normalised to standard solvent conditions (density and viscosity of water at 20.0^{o}C) to yield $s_{20,w}$. Concentration in fringe displacement units were converted to mass concentration, corrected for radial dilution (15).

SEC-MALS-IV

The system consisted of two columns (TOSOH Biosciences TSK 3000 and 4000) and a guard column (TSK Guard TWH) and 3 Wyatt Technology (Santa Barbara, USA) detectors: multi angle light scattering (MALS - Dawn Helios II), differential pressure imbalance

viscometry (ViscoStar) and refractive index concentration measurement (OptiLab rEX). The apparatus was equilibrated with the appropriate buffer for at least 10 hours prior to injection of 100µl of sample. Three GA samples were injected at three concentrations at three ionic strengths. Data were collected and analysed using ASTRA v4 (Wyatt) software. Intrinsic viscosity [η] was evaluated from the relative viscosity η_r yielded by the ViscoStar detector and the mass concentration (c), evaluated from the OptiLab rEX detector, using the Solomon Ciuta (16) equation:

$$[\eta] \cong 1/c\left(2(\eta_r - 1) - 2\ln(\eta_r)\right)^{0.5} \quad (1)$$

Statistical analysis

Linear regression analyses for partial specific volume and sedimentation coefficient evaluations were tested for significance using Analysis of CoVariance (ANCOVA) in GenStat v15 (VSN International). F values are the ratio of regression sum of squares over mean square error. The critical level of significance was set to $p \leq 0.05$.

RESULTS AND DISCUSSION

Density measurement

Partial specific volumes ($\bar{v}$) were calculated using linear regressions of density (ρ) against concentration (c), as described in the following relation (17).

$$\bar{v} = \left(1 - \partial\rho/\partial c\right)/\rho_0 \quad (2)$$

and the results are included in Table 1.

<TABLE 1>

The partial specific volume of the two GA samples ranged between 0.60-0.65ml/g. ANCOVA did not show a significant correlation between the partial specific volume and ionic strength for GAB or GAG ($F_{2,26}$=0.94, P=0.403; $F_{2,21}$=1.01, P=0.382, respectively).

The average value for the partial specific volume was 0.631ml/g, with a standard deviation of 0.013. Typical values for partial specific volume are approximately 0.6ml/g for polysaccharides and 0.73ml/g for proteins. Results in between these two values correlate with the protein content of GA.

Sedimentation velocity

AUC-SV scans were analysed using a ls-g*(s) fit, as shown in Figure 1(a,b). Both showed similar behaviour - the distributions show single peaks at approximately 8S apex, distributed between ~2 and ~30S, and there is a difference between the 0.1M and higher ionic strengths, although not between 0.3 and 0.5M.

Concentration dependence of sedimentation coefficients

Concentration dependence was measured using a linear regression of Equation (3), results of which are shown in Figure 1(c,d) and Table 1. A similar regression, in the form of the reciprocal of sedimentation coefficients plotted against concentration, is more commonly used for other polysaccharides but for near-spherical particles, as posited for GA, the direct plot is preferable (18).

$$s_{20,w} = s^0_{20,w}\left(1 - k_s c\right) \quad (3)$$

The statistical analysis (ANCOVA) showed a significant difference between the concentration dependence of sedimentation coefficients and ionic strength for GAB ($F_{2,14}$=5.57, P=0.017). There was also a significant difference between $s^0_{20,w}$ for 0.3 and 0.5M ionic strength ($F_{1,10}$=11.50, p=0.007). For GAG, although there was a significant dependence between extrapolated sedimentation coefficients for different ionic strengths ($F_{2,15}$=669, p<0.001), there was no significant difference on the concentration dependence ($F_{2,15}$=1.54, p=0.246). There was also a significant difference between $s^0_{20,w}$ values for 0.3 and 0.5M ($F_{1,10}$=18, p=0.002).

<FIGURE 1>

Although for GAB the concentration dependence seems to be dependent on ionic strength, this is not the case for GAG.

SEC-MALS-IV

Figure 2 shows elution times for the three GA samples. The data has been normalised for detector voltage to aid comparison. The molar mass values (principally the weight average but also the number average) obtained are shown in Table 2, along with intrinsic viscosity and hydrated radius (r_H) calculated using Equation 4 - a combination of information of molar mass (M) and intrinsic viscosity [η] (19).

$$r_H = \left(3[\eta]M/10\pi N_A\right)^{1/3} \quad (4)$$

Where N_A is Avogadro's constant. The data show that all six samples eluted at approximately the same time, at ~8 minutes. The highlighted section also shows evidence for

a secondary peak around 14-18 minutes elution time in 0.1M, not present in 0.3 and 0.5M ionic strengths. A similar result was found from AUC-SV where the higher ionic strength preparations were significantly different in distribution to the 0.1M ionic strength. These results suggest that increasing ionic strength decreases the dispersity of size distribution.

<FIGURE 2>

<TABLE 2>

The molecular weight of GAB was determined between 861kDa and 960kDa. For GAG, the weight average molar mass was between 535 and 561kDa. The polydispersity for GAB was higher, at around 1.6, with GAG around 1.3. The intrinsic viscosity obtained through the online pressure imbalance viscometer shows that for GAB, the value ranged between 28.2 and 31.3ml/g. For GAG, this range is lower, between 25.1 and 27.9ml/g. Both GA samples consistently show a reduction in intrinsic viscosity with an increase in ionic strength from 0.1M to 0.3M and above. This suggests that increasing ionic strength makes the GA molecule more compact.

The hydrated radius was calculated as a function of intrinsic viscosity and weight average molar mass. Values for GAB were between 14.7-15.5nm and GAG were between 12.5-13.2nm. This is consistent with both the molar mass and intrinsic viscosity measurements that GAB is the larger sample in terms of mass and size. Although the hydrated radius decreased with ionic strength, the high standard error, and the lack of trend from intrinsic viscosity and molar mass, suggests that this change is not significant. Since the

hydrodynamic radius was a derived value from molar mass and intrinsic viscosity, few conclusions can be drawn from these findings.

Conformational analysis

Wales-van Holde ratio

Concentration dependence of sedimentation coefficients can be combined with intrinsic viscosity data to provide information about the shape/symmetry of the macromolecule. The Wales-van Holde ratio (20) is the ratio between k_s and [η] and provides a hydration-independent shape factor. Table 3 shows $k_s/[\eta]$ values for the GA samples, with intrinsic viscosity values taken from IV results from SEC-MALS. The mean $k_s/[\eta]$ value was (1.5 ±0.2).

MHKS power law analysis

Data from SEC-MALS-IV were analysed for the comparison of molar mass and intrinsic viscosity; the double logarithmic relationship between them being used as a measure of the conformation of the macromolecule. The gradient is defined as the Mark Houwink Kuhn Sakurada (MHKS) shape factor 'a'. Figure 3 shows the plots for all six samples, whilst regression data is summarised in Table 3. Dataset ranges were reduced to appropriate ranges of molar mass.

The MHKS values obtained were consistent with those found in other GPC studies in similar conditions, such as Renard et al. who found a=0.45 (13) and 0.35 (21), Masuelli found 0.55 (at 20°C) (22), Sanchez et al. found 0.46 (19) and Idris et al. found a=0.47 (23).

<FIGURE 3>

Standard errors of the fitted slopes were ≤10%. The intercept consistently had poor error due to the reverse logarithm required to obtain the constant, but this is consistent with other findings (24) and does not greatly affect the reliability of the gradient as the main conformational probe. Less data were obtained from GAG 0.1M compared to others, explaining the low gradient.

<TABLE 3>

Molar mass results from MALS-IV suggested that these gradients should have reduced with increasing ionic strength, however, there was no reliable trend for the shape factor and the ionic strength. Average values between 0.43 and 0.48 represent a conformation between a compact sphere (≈0) and a random coil (≈0.5-0.8), although closer to random coil.

Ellipsoid modelling

Data from AUC-SV and SEC-MALS-IV were used to estimate the molecular dimension and axial ratio of the GA samples using SingleHydFit v3 (25) and shown in Table 3. The swollen specific volume was estimated from the average Wales-van Holde ratio (a hydration-independent shape factor) of 1.5 converted to axial ratio using the FORTRAN package ELLIPS suite (26). The viscosity increments (ν) were obtained from ELLIPS to estimate the swollen volume (V_s) using the following equation (27):

$$[\eta] = \nu \cdot V_S \tag{5}$$

The time-averaged hydration δ (g water / g macromolecule) was estimated using Eq. 6 (27). The hydration ranged between 8.5-10.5g/g, which is a higher estimate than some previous findings (4g/g) (28) but consistent with others (9g/g, 20^{o}C) (22).

$$V_S = \bar{v} + \delta/\rho_0 \quad (6)$$

The graphical outputs from SingleHydFit are displayed in Figure 4. A summary of the fitted parameters is shown in Table 3 including estimations for the error of the model.

From these data, an ellipsoid was plotted using MATLAB R2014a (The MathWorks Inc, Mass. USA). These are depicted in Figure 5. These estimates are somewhat different to previously published results (19), which included a sedimentation coefficient of 0.24S, almost two orders of magnitude lower than what we have found in the present study.

<FIGURE 4>

<FIGURE 5>

There appears to be a reduction in axial ratio and decrease in dimension with increasing ionic strength from both sources. This is in agreement with findings from MALS-IV, where the intrinsic viscosity decreased with increasing ionic strength. Although Figure 5 depicts a single prolate ellipsoid, a more likely scenario is a distribution of axial ratio/dimension as seen from the lightest contours in Figure 4, based on the distribution of molar masses. i.e., lower molar mass species of GA will have smaller dimension and a lower axial ratio.

Increasing ionic strength will force the entire distribution further down this contour map, as observed in Figure 4.

Branwell samples showed a higher axial ratio than Glycomix, possibly because of the higher weight average molar mass. What this would suggest is an arrangement that the polysaccharide collapses in on itself as the charge density builds. Increasing the ionic strength suppresses these charges and the macromolecule relaxes into a slightly more spherical shape.

Conclusions

GA is a commercially important non-dietary fibre with applications in the food and pharmaceutical industries as a stabiliser and drug delivery vector. Two sources were characterised using complementary hydrodynamic techniques including AUC-SV, SEC-MALS-IV and density measurement. Partial specific volume was measured as 0.635ml/g, with no dependence on ionic strength. AUC-SV and SEC-MALS-IV found that increasing ionic strength increased the sedimentation coefficient and decreased the intrinsic viscosity, respectively. Compiled results obtained through these hydrodynamic techniques were able to yield an estimate for the ellipsoid structure of GA using SingleHydFit, in the form of a prolate ellipsoid with an average axial ratio of 1.9 with some indication of a reduction with increase in ionic strength. This form of hydrodynamic modelling is not just applicable for polysaccharides, but other biopolymers and synthetic polymers.

AUTHOR INFORMATION

Corresponding Author

* Corresponding author email address: richard.gillis@nottingham.ac.uk

Author Contributions

The manuscript was written through contributions of all authors. All authors have given approval to the final version of the manuscript.

Funding Sources

This research was funded by the BBSRC.

AUTHOR CONTRIBUTIONS

Richard Gillis: Performed research, analysed data, wrote the paper

Gary Adams: Analysed data, designed research

Qushmua Alzahrani: Performed research, analysed data

Stephen Harding: Analysed data, designed research

ACKNOWLEDGMENT

The authors wish to thank Professor Arthur Rowe for his input on hydrodynamic analysis and theory.

ABBREVIATIONS

AUC, Analytical Ultracentrifugation; GA, Gum Arabic; [η], Intrinsic viscosity; ls-g*(s), least square apparent Gaussian distribution of sedimentation coefficients; N_A, Avogadro's constant; SEC-MALS-DPIV, Size Exclusion Chromatography coupled to Multi Angle Light Scattering and Differential Pressure Imbalance Viscometer; s, Sedimentation coefficient; SV, Sedimentation Velocity.

REFERENCES

1. D. Verbeken, S. Dierckx, K. Dewettinck, Appl Microbiol Biot 2003, 63, 10-21.

2. M. Evans, I. Ratcliffe, P. A. Williams, Curr Opin Colloid Interface Sci 2013, 18, 272-282.

3. B. H. Ali, A. Ziada, G. Blunden, Food Chem Toxicol 2009, 47, 1-8.

4. S. P. Nie, C. Wang, S. W. Cui, Q. Wang, M. Y. Xie, G. O. Phillips, Food Hydrocolloid 2013, 32, 221-227.

5. S. P. Nie, C. Wang, S. W. Cui, Q. Wang, M. Y. Xie, G. O. Phillips, Food Hydrocolloid 2013, 31, 42-48.

6. T. Mahendran, P. Williams, G. Phillips, S. Al-Assaf, T. Baldwin, J Agric Food Chem 2008, 56, 9269-9276.

7. W. Qi, C. Fong, D. T. Lamport, Plant Physiol 1991, 96, 848-855.

8. M. Andres-Brull, S. Al-Assaf, G. O. Phillips, K. Jackson, Analytical Methods 2013, 5, 4047-4052.

9. J. Alftrén, J. M. Peñarrieta, B. Bergenståhl, L. Nilsson, Food Hydrocolloid 2012, 26, 54-62.

10. F. Goycoolea, E. Morris, R. Richardson, A. Bell. Carbohydr Polym 1995, 27, 37-45.

11. T. Funami, M. Nakauma, S. Noda, S. Ishihara, I. Asai, N. Inouchi, K. Nishinari, Food hydrocolloid 2008, 22, 1528-1540.

12. M. Huglin, J. Brandrup, E. Immergut, Polymer handbook; Wiley: New York, 1989.

13. D. Renard, E. Lepvrier, C. Garnier, P. Roblin, M. Nigen, C. Sanchez, Carbohydr Polym 2014, 99, 736-747.

14. P. Schuck, P. Rossmanith, Biopolymers 2000, 54, 328-341.

15. S. E. Harding, G. G. Adams, F. Almutairi, Q. Alzahrani, T. Erten, M. S. Kok, R. B. Gillis, Methods Enzymol 2015, 562, 391-439

16. O. Solomon, I. Ciuta, J. Appl Polym Sci 1962, 6, 683-686.

17. O. Kratky, H. Leopold, H. Stabinger, Methods in Enzymol 1973, 27, 98-110.

18. A. J. Rowe, In Analytical ultracentrifugation in biochemistry and polymer science; S. E. Harding, A. J. Rowe, J. C. Horton, Eds.; Royal Society of Chemistry: Cambridge, UK, 1992 pp 394-406.

19. C. Sanchez, C. Schmitt, E. Kolodziejczyk, A. Lapp, C. Gaillard, D. Renard, Biophys J 2008, 94, 629-639.

20. M. Wales, K. Van Holde, J Polym Sci 1954, 14, 81-86.

21. D. Renard, C. Garnier, A. Lapp, C. Schmitt, C. Sanchez, Carbohydr Polym 2012, 90, 322-332.

22. M. A. Masuelli, Am. J Food Sci Tech 2013, 1, 60-66.

23. O. Idris, P. Williams, G. Phillips, Food Hydrocolloid 1998, 12, 379-388.

24. R. B. Gillis, G. G. Adams, B. Wolf, M. Berry, T. M. Besong, A. Corfield, M. S. Kök, R. Sidebottom, D. Lafond, A. J. Rowe, S. E. Harding, Carbohydr Polym 2013, 93, 178-183.

25. A. Ortega, J. García de la Torre, Biomacromolecules 2007, 8, 2464-2475.

26. S. E. Harding, J. C. Horton, H. Colfen, Eur. Biophys J 1997, 25, 347-360.

27. S. E. Harding, Prog Biophys Mol Biol 1997, 68, 207-262.

28. G. Phillips, S. Takigami, M. Takigami. Food Hydrocolloid 1996, 10, 11-19.

FIGURE LEGENDS

Figure 1

Comparison of sedimentation velocity behaviour of GAB (a,c) and GAG (b,d). (a,b) normalised sedimentation coefficient distributions (ls-g*(s) vs. s) analysis of GA (lowest concentration shown); (c,d) integrated peaks of entire concentration series extrapolating to infinite dilution.

Figure 2

Normalised elution profiles of gum arabic at different ionic strength. The elution times for 12-24 minutes have been expanded to highlight secondary smaller peaks. (a) GAB at I=0.1M, (b) GAB at I=0.3M, (c) GAB at I=0.5M, (d) GAG at I=0.1M, (e) GAG at I=0.3M, (f) GAG at I=0.5M.

Figure 3

MHKS analysis of GA at three ionic strengths using linear regression of the logarithms of intrinsic viscosity and weight average molar mass. (a) GAB, (b) GAG.

Figure 4

Output from SingleHydFit for GA at three ionic strengths with model error reported as 1-3* (1* >10% error; 2* 5-10%; 3* <5%). (a) GAB at I=0.1M, (b) GAB at I=0.3M, (c) GAB at I=0.5M, (d) GAG at I=0.1M, (e) GAG at I=0.3M, (f) GAG at I=0.5M.

Figure 5

Prolate ellipsoid representations for GA at three ionic strengths. (a) GAB at I=0.1M, (b) GAB at I=0.3M, (c) GAB at I=0.5M, (d) GAG at I=0.1M, (e) GAG at I=0.3M, (f) GAG at I=0.5M.

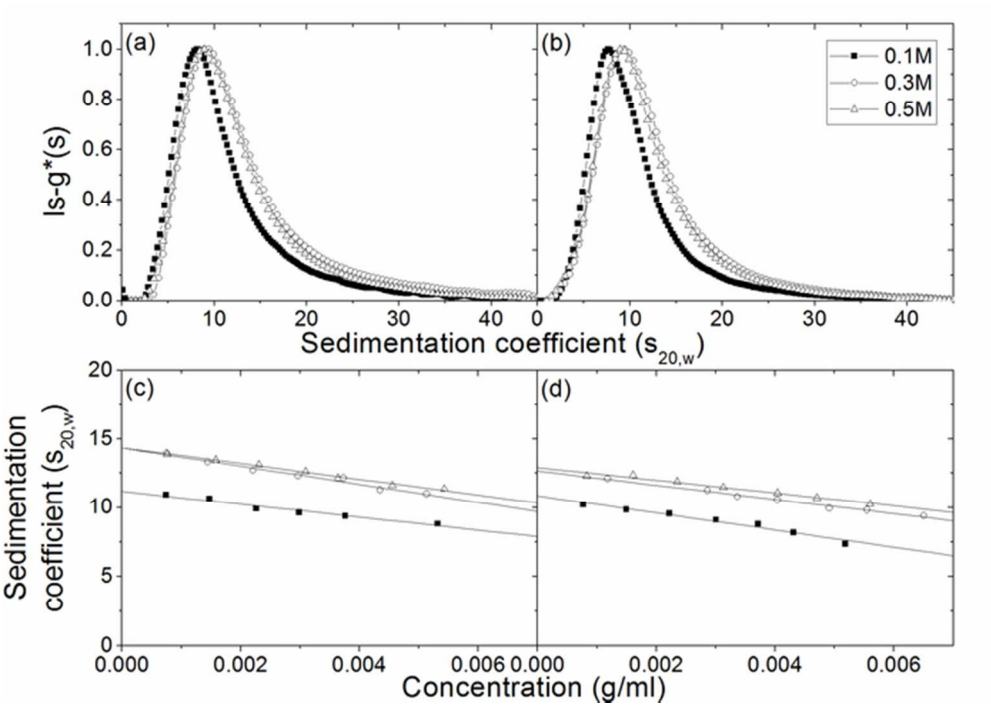

Comparison of sedimentation velocity behaviour of GAB (a,c) and GAG (b,d). (a,b) normalised sedimentation coefficient distributions (ls-g*(s) vs. s) analysis of GA (lowest concentration shown); (c,d) integrated peaks of entire concentration series extrapolating to infinite dilution.
59x41mm (300 x 300 DPI)

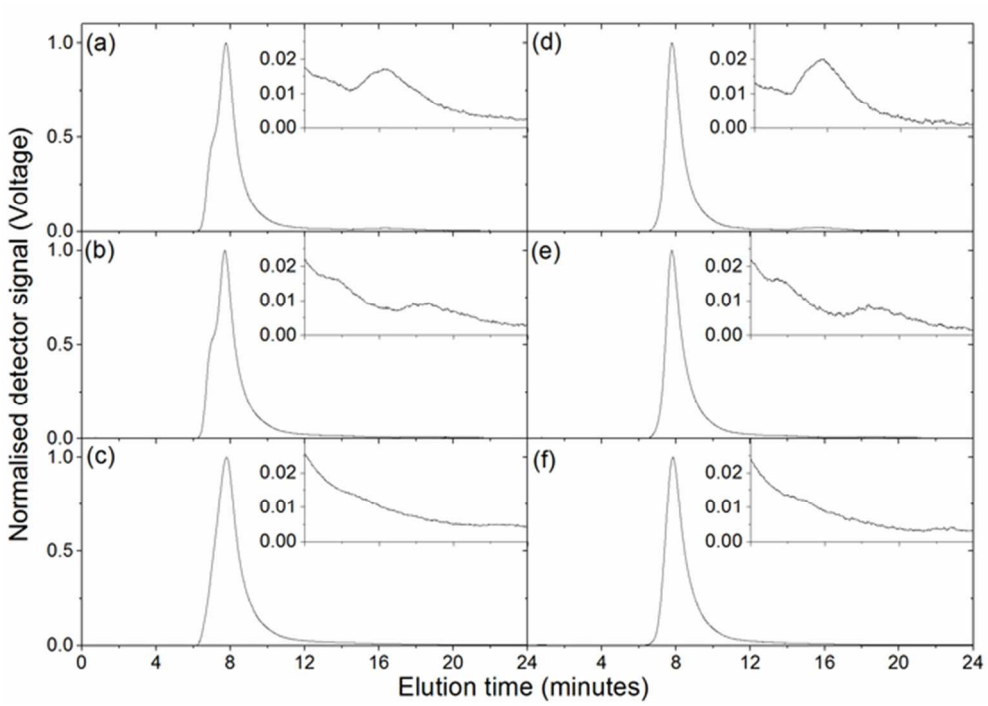

Normalised elution profiles of gum arabic at different ionic strength. The elution times for 12-24 minutes have been expanded to highlight secondary smaller peaks. (a) GAB at I=0.1M, (b) GAB at I=0.3M, (c) GAB at I=0.5M, (d) GAG at I=0.1M, (e) GAG at I=0.3M, (f) GAG at I=0.5M.
59x41mm (300 x 300 DPI)

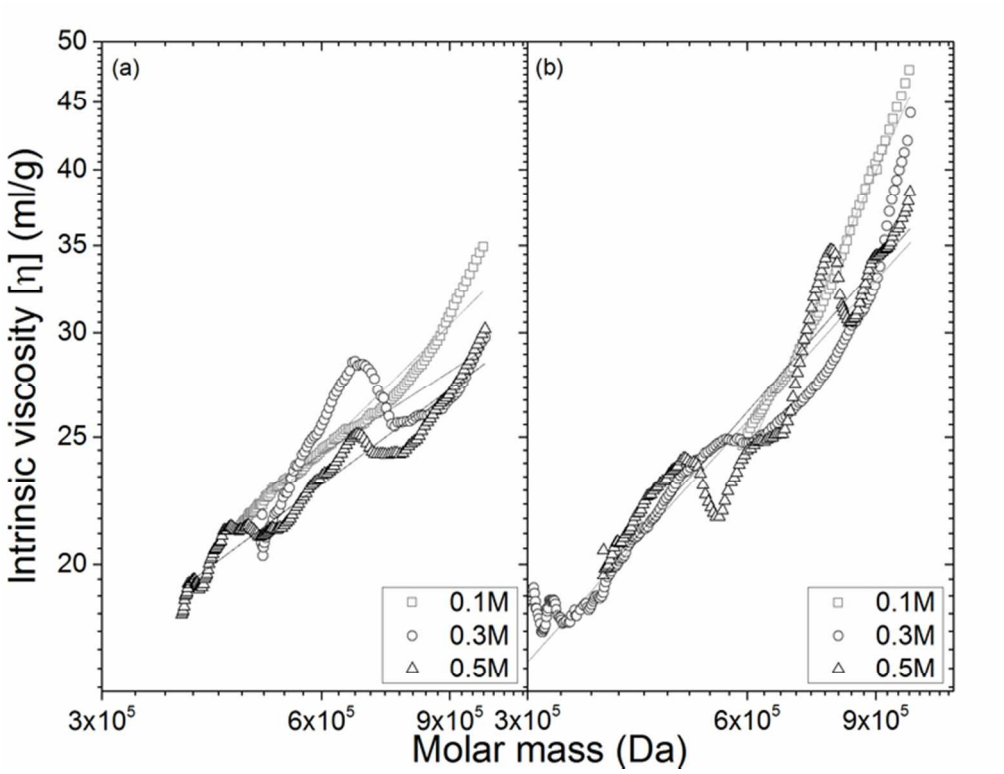

MHKS analysis of GA at three ionic strengths using linear regression of the logarithms of intrinsic viscosity and weight average molar mass. (a) GAB, (b) GAG.
65x49mm (300 x 300 DPI)

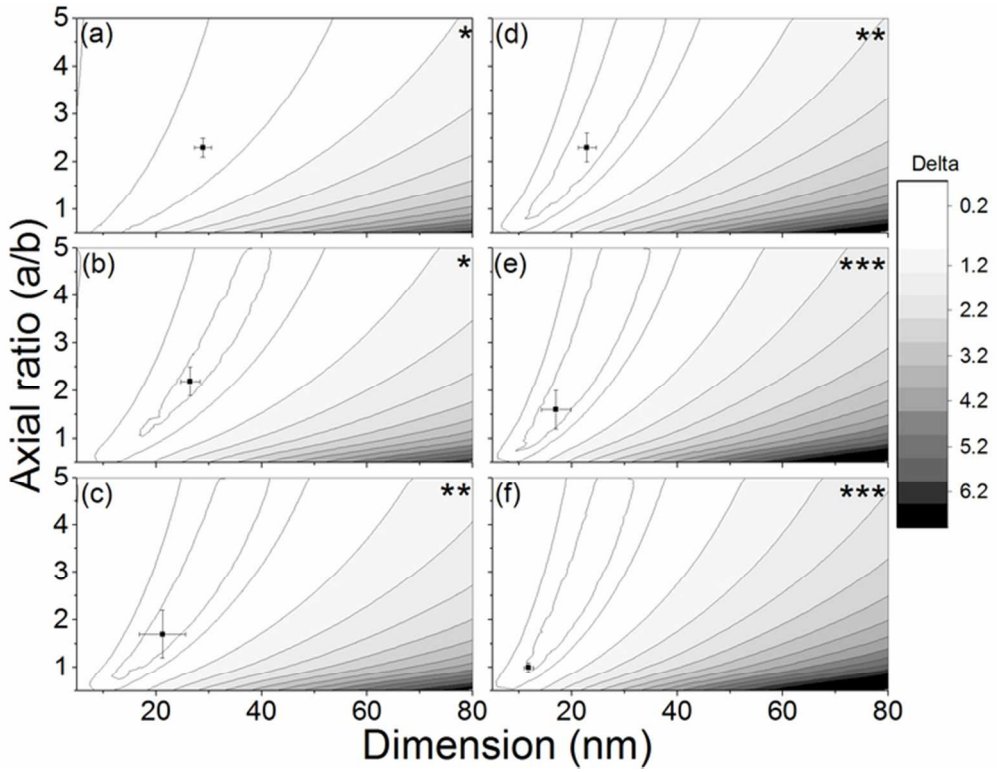

Output from SingleHydFit for GA at three ionic strengths with model error reported as 1-3* (1* >10% error; 2* 5-10%; 3* <5%). (a) GAB at I=0.1M, (b) GAB at I=0.3M, (c) GAB at I=0.5M, (d) GAG at I=0.1M, (e) GAG at I=0.3M, (f) GAG at I=0.5M.
65x49mm (300 x 300 DPI)

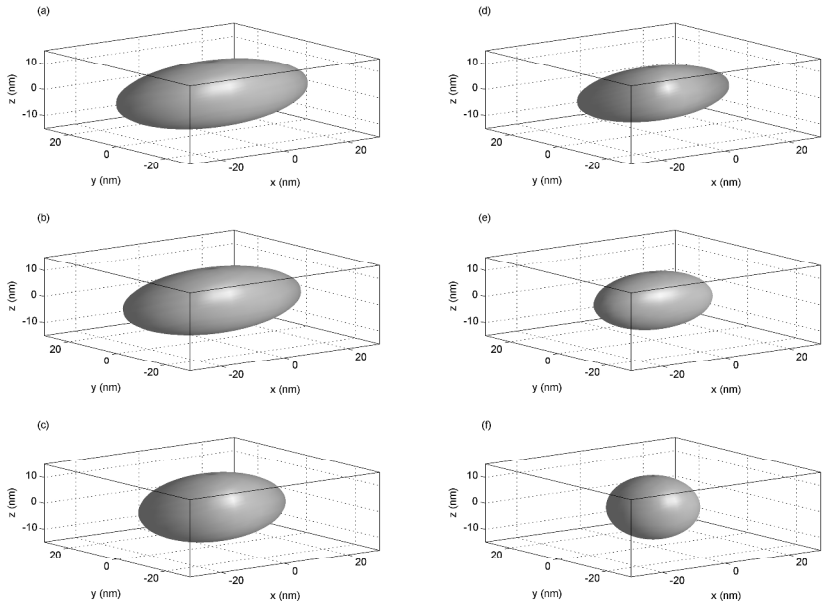

Prolate ellipsoid representations for GA at three ionic strengths. (a) GAB at I=0.1M, (b) GAB at I=0.3M, (c) GAB at I=0.5M, (d) GAG at I=0.1M, (e) GAG at I=0.3M, (f) GAG at I=0.5M.
338x233mm (300 x 300 DPI)

TABLE LEGENDS

Table 1
Partial specific volume and sedimentation velocity for preparations of GAB and GAG in different ionic strengths.

Table 2
Molar mass and intrinsic viscosity data from SEC-MALS-IV of gum Arabic at different ionic strengths.

Table 3
Conformational analysis of GA, at three ionic strengths, using three independent methods.

Table 1: Partial specific volume and sedimentation velocity for preparations of GAB and GAG in different ionic strengths.

Sample	Ionic Strength (M)	$\bar{v}$ (ml/g)	$s^0_{20,w}$ x10^{13} (S)	k_s (ml/g)
GAB	0.1	0.633	11.2 ±0.1	42 ±5
	0.3	0.607	14.3 ±0.2	46 ±4
	0.5	0.636	14.4 ± 0.1	40 ±2
GAG	0.1	0.629	11.2 ±0.1	45 ±3
	0.3	0.631	13.4 ±0.1	39 ±1
	0.5	0.647	14.0 ±0.2	42 ±4

Table 2: Molar mass and intrinsic viscosity data from SEC-MALS-IV of gum Arabic at different ionic strengths.

Sample	Ionic Strength (M)	M_w (kDa)	M_n (kDa)	w/n PDI	[η] (ml/g)	r_H (nm)
GAB	0.1	951 ±12	599 ±5	1.59 ±0.03	31.3 ±0.4	15.5 ±0.1
	0.3	960 ±13	576 ±5	1.60 ±0.03	28.2 ±1.0	15.0 ±0.1
	0.5	861 ±10	548 ±5	1.57 ±0.02	28.4 ±0.8	14.7 ±0.1
GAG	0.1	561 ±5	456 ±5	1.23 ±0.02	27.9 ±1.6	13.2 ±0.2
	0.3	547 ±4	421 ±5	1.30 ±0.02	25.1 ±1.4	12.6 ±0.2
	0.5	536 ±4	424 ±4	1.26 ±0.02	25.1 ±4.3	12.5 ±0.6

PDI: Polydispersity index (ratio of weight over number average molar mass)

Table 3: Conformational analysis of GA, at three ionic strengths, using three independent methods.

Sample	Ionic Strength (M)	Wales-van Holde	MHKS	SingleHydFit	
		$k_s/[\eta]$	a	d	a/b
GAB	0.1	1.3 ±0.2	0.54 ±0.01	29 ±2	2.3 ±0.2
	0.3	1.6 ±0.1	0.35 ±0.03	27 ±2	2.2 ±0.3
	0.5	1.4 ±0.1	0.41 ±0.01	21 ±4	1.7 ±0.5
GAG	0.1	1.6 ±0.1	0.10 ±0.01	23 ±2	2.3 ±0.3
	0.3	1.6 ±0.1	0.63 ±0.01	17 ±3	1.6 ±0.4
	0.5	1.7 ±0.2	0.34 ±0.03	12 ±1	1.0 ±0.1

TABLE LEGENDS

Table 1
Partial specific volume and sedimentation velocity for preparations of GAB and GAG in different ionic strengths.

Table 2
Molar mass and intrinsic viscosity data from SEC-MALS-IV of gum Arabic at different ionic strengths.

Table 3
Conformational analysis of GA, at three ionic strengths, using three independent methods.

Table 1: Partial specific volume and sedimentation velocity for preparations of GAB and GAG in different ionic strengths.

Sample	Ionic Strength (M)	$\bar{v}$ (ml/g)	$s^0_{20,w}$ x10^{13} (S)	k_s (ml/g)
GAB	0.1	0.633	11.2 ±0.1	42 ±5
	0.3	0.607	14.3 ±0.2	46 ±4
	0.5	0.636	14.4 ± 0.1	40 ±2
GAG	0.1	0.629	11.2 ±0.1	45 ±3
	0.3	0.631	13.4 ±0.1	39 ±1
	0.5	0.647	14.0 ±0.2	42 ±4

Table 2: Molar mass and intrinsic viscosity data from SEC-MALS-IV of gum Arabic at different ionic strengths.

Sample	Ionic Strength (M)	M_w (kDa)	M_n (kDa)	w/n PDI	[η] (ml/g)	r_H (nm)
GAB	0.1	951 ±12	599 ±5	1.59 ±0.03	31.3 ±0.4	15.5 ±0.1
	0.3	960 ±13	576 ±5	1.60 ±0.03	28.2 ±1.0	15.0 ±0.1
	0.5	861 ±10	548 ±5	1.57 ±0.02	28.4 ±0.8	14.7 ±0.1
GAG	0.1	561 ±5	456 ±5	1.23 ±0.02	27.9 ±1.6	13.2 ±0.2
	0.3	547 ±4	421 ±5	1.30 ±0.02	25.1 ±1.4	12.6 ±0.2
	0.5	536 ±4	424 ±4	1.26 ±0.02	25.1 ±4.3	12.5 ±0.6

PDI: Polydispersity index (ratio of weight over number average molar mass)

Table 3: Conformational analysis of GA, at three ionic strengths, using three independent methods.

Sample	Ionic Strength (M)	Wales-van Holde	MHKS	SingleHydFit	
		$k_s/[\eta]$	a	d	a/b
GAB	0.1	1.3 ±0.2	0.54 ±0.01	29 ±2	2.3 ±0.2
	0.3	1.6 ±0.1	0.35 ±0.03	27 ±2	2.2 ±0.3
	0.5	1.4 ±0.1	0.41 ±0.01	21 ±4	1.7 ±0.5
GAG	0.1	1.6 ±0.1	0.10 ±0.01	23 ±2	2.3 ±0.3
	0.3	1.6 ±0.1	0.63 ±0.01	17 ±3	1.6 ±0.4
	0.5	1.7 ±0.2	0.34 ±0.03	12 ±1	1.0 ±0.1